Ninth International Conference on Fast Sea Transportation
FAST2007, Shanghai, China, September 2007

Validation of a 4DOF Manoeuvring Model of a High-speed Vehicle-Passenger Trimaran

Tristan Perez[1], Tim Mak[2], Tony Armstrong[2], Andrew Ross[1], and Thor I. Fossen[3]

[1]Centre for Ships and Ocean Structures (CeSOS), Norwegian University of Science and Technology, Trondheim NO-7491, NORWAY.

[2]Austal Development Project Team (ADePT), Austal Ships, Henderson 6166, Western Australia

[3]Department of Engineering Cybernetics, Norwegian University of Science and Technology, Trondheim NO-7491, NORWAY.

ABSTRACT

This paper presents the validation of a manoeuvring model for a novel 127m-vehicle-passenger trimaran via full scale trials. The adopted structure of the model is based on a model previously proposed in the literature with some simplifications. The structure of the model is discussed. Then initial parameter estimates are computed, and the final set of parameters are obtained via adjustments based on engineering judgement and application of a genetic algorithm so as to match the data of the trials. The validity of the model is also assessed with data from a trial different from the one use for the parameter adjustment. The model shows good agreement with the trial data.

KEYWORDS

Manoeuvring, High-speed, Trimaran, Hydrodynamics

1 INTRODUCTION

Austal's hull design H260 (shown in Figure 1), is the result of pursuing improved passenger comfort and economy, which has improved fast ferry sea transportation beyond the ability of contemporary designs (Armstrong 2006). Two of the key aspects of the design have been good seakeeping and low resistance.

In this paper, a characterization of its manoeuvring capabilities is assessed via manoeuvring modelling in 4 degrees of freedom (DOF). The approach taken to obtain the model is a grey-box one; i.e., a model structure is adopted based on first principles and combined with initial parameter estimates and adjustments by genetic algorithm so as to match the sea trials data. The rest of the paper describes the model, the initial parameter estimates and provides a discussion of the results obtained.

2 MODELLING

Following Fossen (2002), a compact representation of a manoeuvring model of a high-speed can be written as

$$\begin{aligned} \dot{\boldsymbol{\eta}} &= \mathbf{J}(\boldsymbol{\eta})\,\boldsymbol{\nu} \\ \mathbf{M}\,\dot{\boldsymbol{\nu}} + \mathbf{C}(\boldsymbol{\nu})\,\boldsymbol{\nu} + \mathbf{D}(\boldsymbol{\nu})\,\boldsymbol{\nu} + \mathbf{G}(\boldsymbol{\eta}) &= \boldsymbol{\tau} \end{aligned} \tag{1}$$

These equations of motion are formulated about the origin of a coordinate system fixed the vessel (body-fixed frame). For this vessel, the adopted coordinate system is fixed to the point determined by the intersection of the port-starboard plane of symmetry, the waterline plane and a transverse vertical plane at *Lpp/2*. The positive convention corresponds to SNAME: forward-starboard-down.

The vector variables in the model (1) are defined as follows:

$$\begin{aligned} \boldsymbol{\eta} &= [n \quad e \quad \phi \quad \psi]^T \\ \boldsymbol{\nu} &= [u \quad v \quad p \quad r]^T \\ \boldsymbol{\tau} &= [X \quad Y \quad K \quad N]^T \end{aligned} \tag{2}$$

The first vector gives the position *n*–North *e*-East in the local geographical coordinate system and orientation in terms of the roll and heading (yaw) angles. The second vector gives the velocities and rates in body-fixed coordinates, with components of surge speed, sway speed, roll rate and yaw rate respectively. The last vector gives the forces and moments in the DOF (also considered in body-fixed coordinates): *X*-surge force, *Y*-sway force, *K*-roll moment, *N*-yaw moments.

Figure 1: Austal's hull H260 "Benchijigua Express"

2.1 Kinematic Transformation

The kinematic transformation in 4DOF is given by

$$\mathbf{J}(\boldsymbol{\eta}) = \begin{bmatrix} \cos\psi & -\sin\psi\cos\phi & 0 & 0 \\ \sin\psi & \cos\psi\cos\phi & 0 & 0 \\ 0 & 0 & 1 & 0 \\ 0 & 0 & 0 & \cos\phi \end{bmatrix} \tag{3}$$

2.2 Rigid Body and Added Mass

The total mass matrix is composed of a rigid body and added mass term:

$$\mathbf{M} = \mathbf{M}_{RB} + \mathbf{M}_{A}$$

The structure of the rigid body mass depends on the point in which the equation of motion (1) is formulated (origin of the body-fixed frame):

$$\mathbf{M}_{RB} = \begin{bmatrix} m & 0 & 0 & -my_G \\ 0 & m & -mz_G & mx_G \\ 0 & -mz_G & Ixx & -Ixz \\ -my_G & mx_G & -Ixz & Izz \end{bmatrix}$$

The mass of the vessel is denoted by m, I_{jj} and I_{ij} are the moments and product of inertia about the origin of the body-fixed frame, and the coordinates of the centre of gravity (CG) from the point in which the equations are formulated are given by

$$\mathbf{r}_{CG}^{b} = \begin{bmatrix} x_G & y_G & z_G \end{bmatrix}^T$$

The added mass matrix in 4DOF is given by

$$\mathbf{M}_{A} = -\begin{bmatrix} X\dot{u} & 0 & 0 & 0 \\ 0 & Y\dot{v} & Y\dot{p} & Y\dot{r} \\ 0 & K\dot{v} & K\dot{p} & K\dot{r} \\ 0 & N\dot{v} & N\dot{p} & N\dot{r} \end{bmatrix}$$

where the hydrodynamic derivatives are denoted according the SNAME nomenclature and convention.

2.3 Coriolis and Centripetal terms

The Coriolis and Centripetal terms have a component due to the rigid-body mass and another component due to the added mass:

$$\mathbf{C}(\mathbf{v}) = \mathbf{C}_{RB}(\mathbf{v}) + \mathbf{C}_{A}(\mathbf{v}) .$$

Using the kinetic energy of the vessel and Kirchoff's Equations, the rigid-body terms can be expressed as follows (Fossen, 2002):

$$\mathbf{C}_{RB}(\mathbf{v}) = \begin{bmatrix} 0 & 0 & mz_G r & -m(x_G r + v) \\ 0 & 0 & 0 & mu \\ -mz_G r & 0 & 0 & Iyz\, r + Ixy\, p \\ m(x_G r + v) & -mu & -Iyz\, r - Ixy\, p & 0 \end{bmatrix}$$

In a similar fashion and by considering the kinetic energy of fluid, the added-mass terms can be expressed as follows (Fossen, 2002):

$$\mathbf{C}_{RB}(\mathbf{v}) = \begin{bmatrix} 0 & 0 & 0 & a_2 \\ 0 & 0 & 0 & -a_1 \\ 0 & 0 & 0 & 0 \\ -a_2 & a_1 & 0 & 0 \end{bmatrix}$$

with

$$a_1 = X\dot{u}\, u$$
$$a_2 = Y\dot{v}\, v + Y\dot{p}\, p + Y\dot{r}\, r$$

Note that the last row contains the Munk moment:

$$N_{Munk} = (X\dot{u} - Y\dot{v})\, u\, v.$$

2.4 Circulation Effects and Viscous Damping

Slender hulls like H260 experience significant lift effects during manoeuvring. A complete derivation—from first principles—of a lift drag model based on low-aspect-ratio wing theory has been recently derived in Ross et al., (2007). In this paper, we take the simplified approach following Blanke (1981).

The hydrodynamic lift experienced by a semi-displacement hull during manoeuvring can be approximated by that of a small aspect ratio hydrofoil (with 3D corrections):

$$L_h \approx \pi\, \rho\, V^2 T^T \sin\alpha ,$$

where V is the flow ambient velocity relative to the vessel, T is the vessel draft, and the angle of attack of the hull can be computed from the body-fixed speeds:

$$\alpha = -\arcsin\frac{v}{\sqrt{u^2 + v^2}} .$$

By taking the above from the stability frame to the body-fixed frame, the hydrodynamic sway force due to sway can be expressed as

$$Y_v v = \frac{\partial Y}{\partial v} v = -\pi\, \rho\, T^2 u\, v := Yuv\, u\, v .$$

The yaw and roll moment due to this force are given by

$$Nv\, v = l_v\, Yv\, v = -l_v\, \pi\, \rho\, T^2 u\, v := Nuv\, u\, v$$
$$Kv\, v = h_v\, Yv\, v = h_v\, \pi\, \rho\, T^2 u\, v := Kuv\, u\, v$$

This representation is consistent with taking only the 1st order terms derived in Ross et al. (2007). As discussed by Blanke (1981), the lever arms l_v and h_v are normally positive, meaning that the centre of pressure is forward and below CG. This produces a destabilising effect in yaw, in which the sway velocity creates a rate of turn.

In a similar way, a steady yaw rate also gives rise to lift effects since the rate of turns induce a side velocity at the centre of pressure. Therefore,

$$Yr\, r = -\pi\, \rho\, T^2 l_v\, u\, r := Yur\, u\, r$$

and

$$Nr\, r = -\pi\, \rho\, T^2 l_v^{\,2}\, u\, r := Nur\, u\, r$$
$$Kr\, r = -\pi\, \rho\, T^2 h_v\, l_v\, u\, r := Kur\, u\, r$$

Apart from lift, the circulation effects also induced drag in the direction of the flow. By considering only the first order terms, the drag component is

$$Xrv \cdot r \cdot v .$$

Combining terms, the lift-drag induced forces can be expressed as

$$\mathbf{D}_{LD}(\mathbf{v}) = \begin{bmatrix} 0 & 0 & 0 & Xrv\, v \\ 0 & Yuv\, u & 0 & Yur\, u \\ 0 & Kuv\, u & 0 & Kur\, u \\ 0 & Nuv\, u & 0 & Kur\, u \end{bmatrix}.$$

With respect to the viscous effects, the model of Norbin (1971) and the simplifications made by Blanke (1981) is adopted:

$$\mathbf{D}_{NL}(\mathbf{v}) = \begin{bmatrix} X_{|u|u} & 0 & 0 & 0 \\ 0 & Y_{|v|v}|v|+Y_{|r|v}|r| & 0 & Y_{|v|r}|v|+Y_{|r|r}|r| \\ 0 & 0 & K_{|p|p}|p|+Y_p & 0 \\ 0 & N_{|v|v}|v|+N_{|r|v}|r| & 0 & N_{|v|r}|v|+N_{|r|r}|r| \end{bmatrix}$$

Then, the total damping in (1) is the sum of the circulation and viscous components:

$$\mathbf{D}(\mathbf{v}) = \mathbf{D}_{LD}(\mathbf{v}) + \mathbf{D}_{NL}(\mathbf{v})$$

2.5 Roll Restoring Term

The roll restoring term is decoupled from the horizontal motion DOF. Therefore in (1),

$$\mathbf{G}(\eta) = \begin{bmatrix} 0 \\ 0 \\ \rho\, g\, \nabla\, GZ(\phi) \\ 0 \end{bmatrix}$$

where the righting arm is described by an odd polynomial fitted to the intact GZ curve:

$$GZ(\phi) = GMt\ \phi + P(\phi) .$$

3 FORCE GENERATORS

The H260 was designed with one booster waterjet, two steerable water jets and two vertically mounted hydrofoils (T-Max) located 3m forward from the nozzles of the water jets.

The T-max hydrofoils are modelled with standard lift-drag formulae by Wicker and Fehlner (1958), and the effective angle of attack and ambient flow velocity are computed based on the local hull motion.

The model for the water jets is based on that of Perdon (1998). The forces are expressed as functions of thrust and bucket deflection δ :.

$$X_{jet} = T \cdot \cos(\delta)$$
$$Y_{jet} = T \cdot \sin(2 \cdot \delta)$$
$$N_{jet} = x_{jet} \cdot Y_{jet}$$

The thrust T due to the waterjets is expressed as,

$$T = \left(1 - \left|\frac{v + x_{jet} \cdot r}{u}\right|\right) \sqrt{1 - X_{\partial\partial} \cdot \sin(|\delta| \cdot \sqrt{|\delta|}} \cdot T_0$$

where, T_0 is the total thrust at the initial speed on a straight course. The first term allows a reduction in thrust caused by the local sway velocity. The second term expresses the loss in thrust due to bucket deflection.

4 INITIAL PARAMETER ESTIMATES

The initial estimates of the added mass we computed (with inertia terms about CG) using a 2.5D seakeeping code, and taking the low frequency values for sway and yaw and the resonant value for roll. These results were compared with the linear coefficient estimates of Clarke, et al., (1983). The estimates were then expressed in terms of the rigid body mass so the multiplying coefficients could be varied to tune the model:

$$Xu\dot{} = -0.05\ m$$
$$Yv\dot{} = -0.7\ m$$
$$Yp\dot{} = -0.015\ m\ z_G$$
$$Yr\dot{} = -0.5\ m\ x_G$$
$$Kv\dot{} = -0.015\ m\ z_G$$
$$Kp\dot{} = -0.5\ Ixx$$
$$Nv\dot{} = -0.12\ m\ x_G$$
$$Nr\dot{} = -0.8\ Izz$$

For the lift-drag terms the initial estimates of the lever arms were taken as

$$h_v = T/2$$
$$l_v = Lpp/4$$
$$Xrv = 0.33\ m$$

For the viscous damping the following estimates were used:

$$Y_{|v|v} = 0.2\ Yuv$$
$$Y_{|v|r} = 0$$
$$K_{|p|p} = 0$$
$$Nv\dot{} = -0.12\ m\ x_G$$
$$N_{|v|v} = -0.5\ Nuv$$

The linear roll damping was estimated from a second order model and the fact that the non-dimensional damping normally takes values between 0.2 and 0.5:

$$Kp = 2\,\xi\,\sqrt{\rho\ g\ GMt\ \nabla\ (Ixx - Kp\dot{})}$$
$$0.1 \le \xi \le 0.5$$

5 MODEL TUNING AND VALIDATION

The model proposed in Section 2 was implemented in MATLAB-SIMULINK, and the command of the control surfaces recorded during the trials were use to excite the

model. Two trial data sets corresponding to zig-zag tests were considered at 35kt:

- Set 1: T-Max 10-10; Water Jets 20-20
- Set 2: T-Max 10-10; Water Jets 10-10

The trials were conducted off Fremantle Western Australia, in March 2005. The measurements taken included: force generator deflection angles, roll angle and yaw rate, recorded at 30Hz, through the vessels Ride control system which used a Kongsberg MRU6 for motion measurements. Forward speed and GPS position were recorded through the ships Marinelink system at 1Hz. The sea conditions were not ideal as there was some remaining swell, and based on the GPS positioning recording it is suspected that a strong current was also present.

Data processing was done to estimate the sway velocity from the second equation in the kinematic transformation based on approximate derivatives (derivative + LP filtering) of the positions. The roll rate was also estimated from an approximate derivative of the roll angle measurements.

The model was tuned using the data set corresponding to the 20-20 zig-zag test since this seemed to be the one least affected by the environmental conditions. Figures 2 to 4 show a comparison between the model response and the trial data.

Figure 2 shows the vessel track and the commands of the water jets and T-Maxs. Figure 3 shows the velocities. As mentioned above, the sway velocity of the trial was estimated from the kinematic transformation and estimates of the derivatives of the positioning measurements. In Figure 3, we can see that there is a lag in the sway velocity attributed to the off-line filtering used to obtain the estimates. Figure 4 shows the roll and yaw angles. Here we can appreciate the influence of the environment on the roll angle measurements, which in turn, appears in the estimate of roll rate derived from these measurements.

Small adjustments of the initial value of the parameters were performed based on the simulation results:

$$h_v = 0.6\,T/2$$
$$l_v = 1.14\,Lpp/4$$
$$\xi = 0.35$$
$$GMt = 0.9\,GMt_{initial}$$

After these adjustments were made the sensitivity of the response to variations in other parameters was found to be very small. This reflects the fact that the zig-zag test does not have adequate persistence of excitation for the number of parameters in the model. That is, the spectral characteristics of the excitation signals are not rich enough to excite the system dynamics. This was expected since the zig-zag test is not designed for system identification.

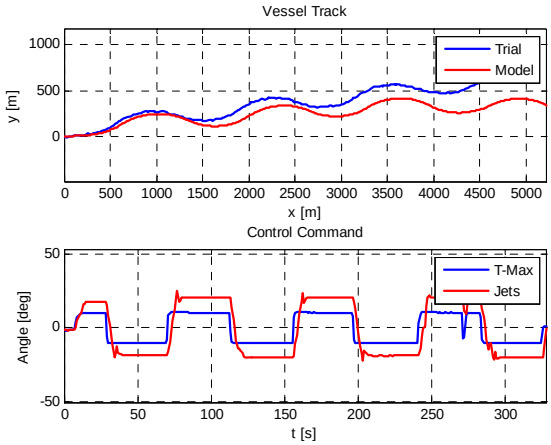

Figure 2: Vessel track and force generator commands during 20-20 zig-zag test

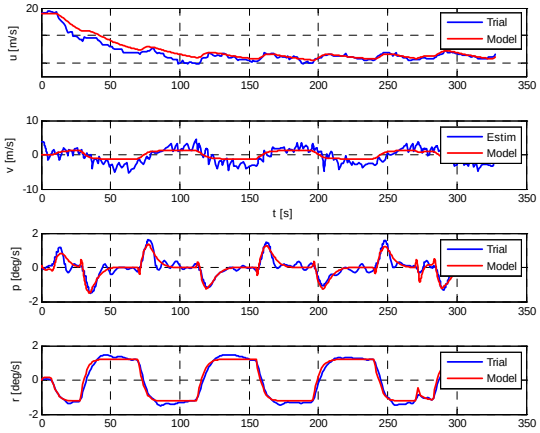

Figure 3: Velocities during the 20-20 zig-zag test

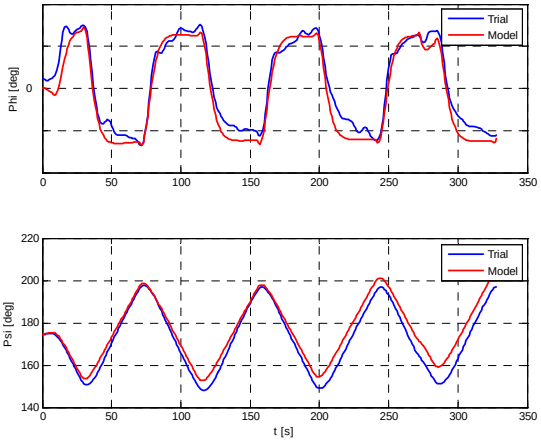

Figure 4: Roll and Yaw angles during the 20-20 zig-zag test

As a measure of performance of how the model reproduces the data, we used the coefficient of determination R^2, which is a statistic that, in this case, can be interpreted as the proportion of the data explained by the model:

$$R^2 = \frac{\sum(\hat{D}-\overline{D})^2}{\sum(\hat{D}-D)^2 + \sum(\hat{D}-\overline{D})^2}$$

where $D, \overline{D}$ represent the measured data and its mean, and $\hat{D}$ the data generated by the model.

A Genetic Algorithm from Passino (2005) was applied to improve the fitness of the model. Then, from the simulations for 20-20 zig-zag test, we have the following results:

- R^2 forward speed: 0.91
- R^2 sway velocity: 0.45
- R^2 roll rate: 0.86
- R^2 yaw rate: 0.97
- R^2 roll angle: 0.94
- R^2 yaw angle: 0.90

These figures show a very good fit of the model to the data of the trials.

The ability of a model to reproduce the same record of data used to adjust the parameters of the model is somehow a trivial validation. Therefore, after fitting the model to the fist data set, a second data set corresponding to a 10-10 zig-zag test was used to test the model without any adjustment of the parameters. Figures 5 and 6 show the corresponding results.

For the second data set we find the following coefficients of determination:

- R^2 forward speed: 0.84
- R^2 sway velocity: 0.46
- R^2 roll rate: 0.85
- R^2 yaw rate: 0.93
- R^2 roll angle: 0.93
- R^2 yaw angle: 0.60

For this data the quality of forward speed, roll angle and yaw rate are largely maintained, whereas the yaw angle quality is reduced.

From Figure 5, we can observe that due to the environmental disturbances, the yaw rate of the trial has lower negative values than the model yaw rate. This produces a trend in the yaw angle shown in Figure 6, and the corresponding decrement of the coefficient of determination. Indeed, by de-trending the yaw angle, we obtain the result shown in Figure 7. This seems to indicate that the difference in heading between the model and the data can be attributed to the environmental disturbances, and that the quality of the model is acceptable.

6 CONCLUSION

In this paper, we have discussed the validation of manoeuvring model in 4DOF based on full scale sea trials. A model was proposed based on existing theory, and initial parameter estimates were obtained from low-frequency seakeeping computations and known results from the literature. A simulation model was implemented and the output of the model compared with the results of the trial while using the same commands to the force generators. Using a set of data, some small parameter adjustments were performed based in engineering judgement. Then a genetic algorithm was applied to improve the fitness of the model. The performance of the model measured by the matching of the model response and data records was very satisfactory.

A validation of the model with a different data set was performed, and satisfactory results were obtained despite some environmental disturbances.

As future work, parameter estimation on a model incorporating more terms and alternative optimisation methods can be considered. However, it is expected that as the number of parameters increase, some of these might not be identifiable using the zig-zag test records. The reason for this is that zig-zag tests are not designed for identification and therefore, it sufficiently exciting given the model structure and the number of parameters.

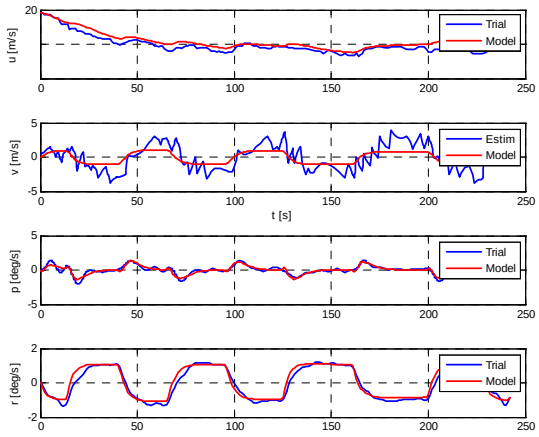

Figure 5: Velocities during the 10-10 zig-zag test

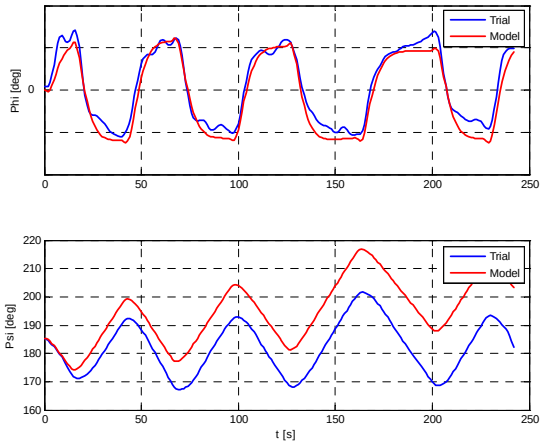

Figure 6: Roll and Yaw during the 10-10 zig-zag test

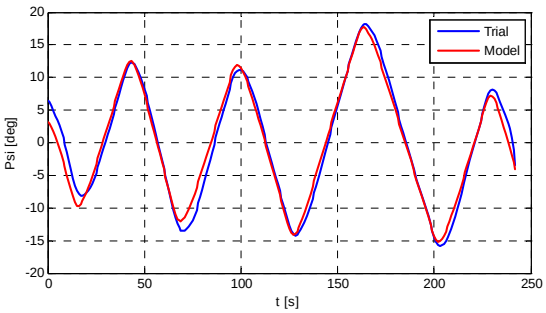

Figure 7: De-trended yaw angle of the 10-10 Zig-Zag test

REFERENCES

Armstrong, N. A., (2006), 'On the performance of a large high-speed trimaran', Australian Journal of Mechanical Engineering Vol 3, No 2.

Blanke, M. (1981), 'Ship propulsion losses related to automatic steering and prime mover control', PhD thesis. Servolaboratory, Technical University of Denmark.

Clarke, D., P. Gedling and G. Hine (1983), 'The application of manoeuvring criteria in hull design using linear theory', The Naval Architect pp. 45–68.

Fossen, T.I. (2002), 'Marine Control Systems: Guidance, Navigation and Control of Ships, Rigs and Underwater Vehicles'. Marine Cybernetics, Trondheim.

Passino, K.M., (2005), 'Biomimicry for Optimization, Control and Automation', Springer-Verlag, London.

Perdon, P., (1998), 'Rotating Arm Manoeuvering Test and Simulation or waterjet propelled Vessels', Proc. International Symposium and Workshop on Force Acting on a Manoeuvring Vessel, September. Val de Reuil, France.

Ross, A., T. Perez and T.I. Fossem (2007), 'A Novel Manoeuvring Model based on Low-spect-ratio Lift Theory and Lagrangian Mechanics', In Proc. IFAC Conference on Control Applications in Marine Systems, Bol, Croatia. September.

Whicker, L.F., and L.F. Fehlner (1958), Free stream characteristics of a family of low aspect ration= control surfaces for applications to ship design. Technical Report 933 DTRC.